Crimson Publishers
Wings to the Research

Research Article

A New Method of Coupled Eulerian-Lagrangian (CEL) to Optimization Underwater Friction Stir Welding with Stationary Shoulder Process of AA6061-T6 Welded Plate

Alireza Fallahi Arezoudar[1] and Akbar Hosseini[2]*

[1]Professor, Department of Mechanical Engineering, Amirkabir University, Iran

[2]PHD, Department of Mechanical Engineering, Amirkabir University, Iran

ISSN: 2832-4463

***Corresponding author:** Akbar Hosseini, PHD, Department of Mechanical Engineering, Amirkabir University, Iran

Submission: February 16, 2026
Published: May 15, 2026

Volume 5- Issue 3

How to cite this article: Alireza Fallahi Arezoudar and Akbar Hosseini*, A New Method of Coupled Eulerian-Lagrangian (CEL) to Optimization Underwater Friction Stir Welding with Stationary Shoulder Process of AA6061-T6 Welded Plate. COJ Rob Artificial Intel. 5(3). COJRA. 000612. 2026.
DOI: 10.31031/COJRA.2026.05.000612

Abstract

Achieving high-integrity AA6061-T6 welded joints requires precise control over microstructural evolution and residual stresses. This study introduces a simulation-driven control method using the Coupled Eulerian-Lagrangian (CEL) framework to optimize Underwater Stationary Shoulder Friction Stir Welding (USSFSW) parameters for target properties. Results show that conventional UFSW produces asymmetric stress distributions, high temperatures, and welding flash due to shoulder-induced extrusion. In contrast, USSFSW generates symmetric stress fields, lower peak temperatures, and eliminates flash via localized pin-driven heat input. Residual stress analysis reveals lower longitudinal/transverse stresses with compressive regions, enhancing mechanical performance. Mechanical testing confirms USSFSW improves yield strength, ultimate tensile strength and joint efficiency by 27%, 18% and 14% respectively, albeit with reduced elongation. Strong agreement between simulated thermal fields, defect predictions, and experiments validates the CEL model. These findings establish USSFSW as superior for thermal-sensitive applications requiring high strength, low distortion, and defect-free welds..

Keywords: Thermo-mechanical simulation; Coupled eulerian-lagrangian; Friction stir welding; Stationary shoulder; Underwater welding, Residual stress distribution

Introduction

Friction Stir Welding (FSW) has emerged as a transformative solid-state joining technology for aluminum alloys, enabling high-strength, low-distortion welds without solidification defects [1]. However, a decade of research has consistently shown that conventional FSW is constrained by substantial frictional heat from the rotating shoulder [2-4]. This induces coarse grain structures, dissolution of strengthening precipitates (particularly in heat-treatable alloys like AA6xxx series) and asymmetric tensile residual stresses that accelerate fatigue failure [5,6]. To address these thermal limitations, two modified variants have been developed and extensively studied. Underwater FSW (UFSW), where the workpiece is submerged in a cooling medium, uses rapid quenching to refine microstructure and reduce peak temperatures [7,8].

Recent work by Selvaraj et al. [9] demonstrated that UFSW of AA7075/Pure Copper reduced grain size by 40% compared to conventional FSW, but noted that the rotating shoulder still created a steep thermal gradient across the weld nugget. Concurrently, Stationary Shoulder FSW (SSFSW) has emerged as an alternative strategy, where a non-rotating shoulder localizes heat generation to the pin, minimizing the thermal input and through-thickness temperature gradients [10,11]. Baghdadchi et al. [12] quantified that SSFSW reduces the total Heat-Affected Zone (HAZ) width by up to 60% in aluminum alloys relative to conventional FSW, though they reported challenges with tool wear at higher traverse speeds. The synergistic combination of these two cooling strategies-Underwater Stationary Shoulder FSW (USSFSW) -has only recently been investigated, with initial studies demonstrating exceptional improvements.

Specifically, for AA6061-T6, USSFSW has been shown to produce finer, symmetric microstructures, compressive residual stress fields and enhanced wear resistance compared to either UFSW or SSFSW alone [13].

Advanced numerical modeling using the Coupled Eulerian-Lagrangian (CEL) method has proven instrumental in capturing the complex thermo-mechanical phenomena governing these processes. Recent implementations by Hosseini et al. [14] incorporated temperature-dependent friction coefficients, showing that CEL predictions of temperature fields in UFSW matched experiments within 5% error. As a result, the CEL method has achieved high-fidelity predictions of temperature fields, material flow, and defect formation in USSFSW [15]. Nevertheless, a critical gap persists: current modeling efforts remain predominantly explanatory rather than prescriptive. While CEL simulations accurately replicate experimental outcomes and validate process superiority, they have not been systematically employed as design tools to proactively identify optimal processing parameters that satisfy multi-objective performance targets. Parameter selection thus remains empirically driven, reliant on costly trial campaigns.

To address this gap, the present paper consolidates and synthesizes a previously developed CEL-based optimization framework for USSFSW of AA6061-T6, drawing upon experimentally validated models established in prior work [13,15]. By defining a multi-objective function encompassing minimized tensile residual stress, maximized post-weld strength and defect-free integrity, the validated CEL model is repurposed from an analytical instrument into a prescriptive design engine. This framework systematically interrogates the process parameter space (rotational speed, traverse speed, water flow rate, pin geometry) to identify optimal parameter sets that minimize the objective function, thereby enabling simulation-driven process control. The approach constitutes a paradigm shift from post-hoc analysis to a priori optimization, offering a rigorous, physics-based pathway for certifying weld performance in industrial applications. This paper presents the architecture of this framework, its experimental validation and its application to demonstrate the superiority of USSFSW over conventional UFSW across thermal, mechanical, and defect-resistance metrics.

Technical Novelty and Research Objectives

While prior work by the authors successfully developed and experimentally validated a CEL model for USSFSW of AA6061-T6 [13,15], those studies were fundamentally explanatory in nature. They demonstrated that the CEL model could accurately replicate experimental results-including temperature history with RMSE < 12 °C for USSFSW (Figure 1b), peak temperature reduction from 525.2 °C to 404.7 °C (Table 1), joint efficiency improvement from 77% to 91% (Table 1), residual stress distribution with maximum error of ~9% (Figure 2a) and defect prediction via EVF (Figure 3). However, the validated model was not systematically employed as a design tool to proactively answer: "Which combination of rotational speed, traverse speed, and cooling conditions simultaneously minimizes tensile residual stress, maximizes post-weld strength, and suppresses defects such as flashes?"

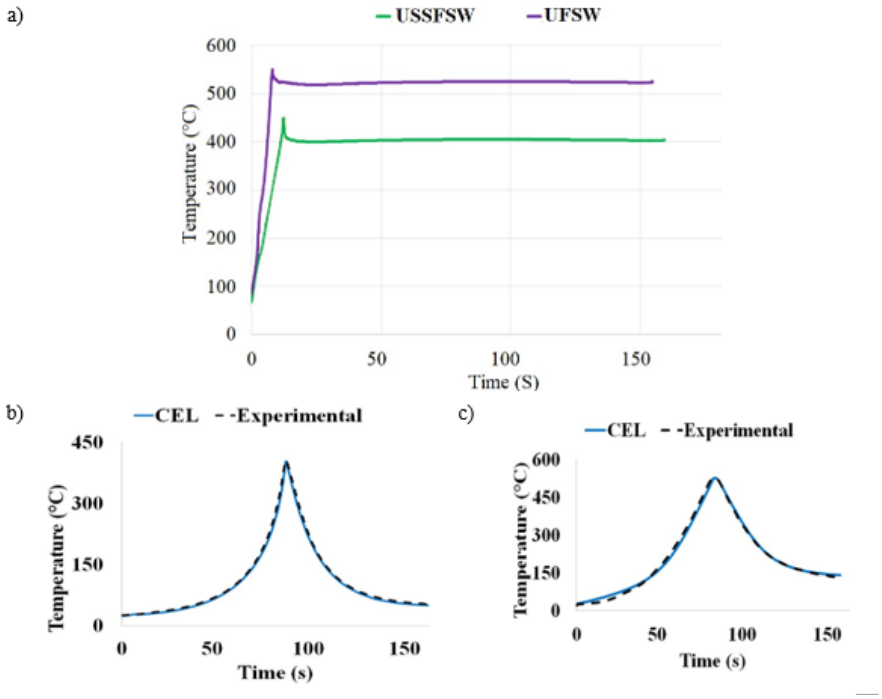

Figure 1: a) Longitudinal temperature distrbution during the USSFSW and UFSW processes, and validation of simulation results with experimental temperature measurement under the joint line for sample b) USSFSW and c) UFSW [15].

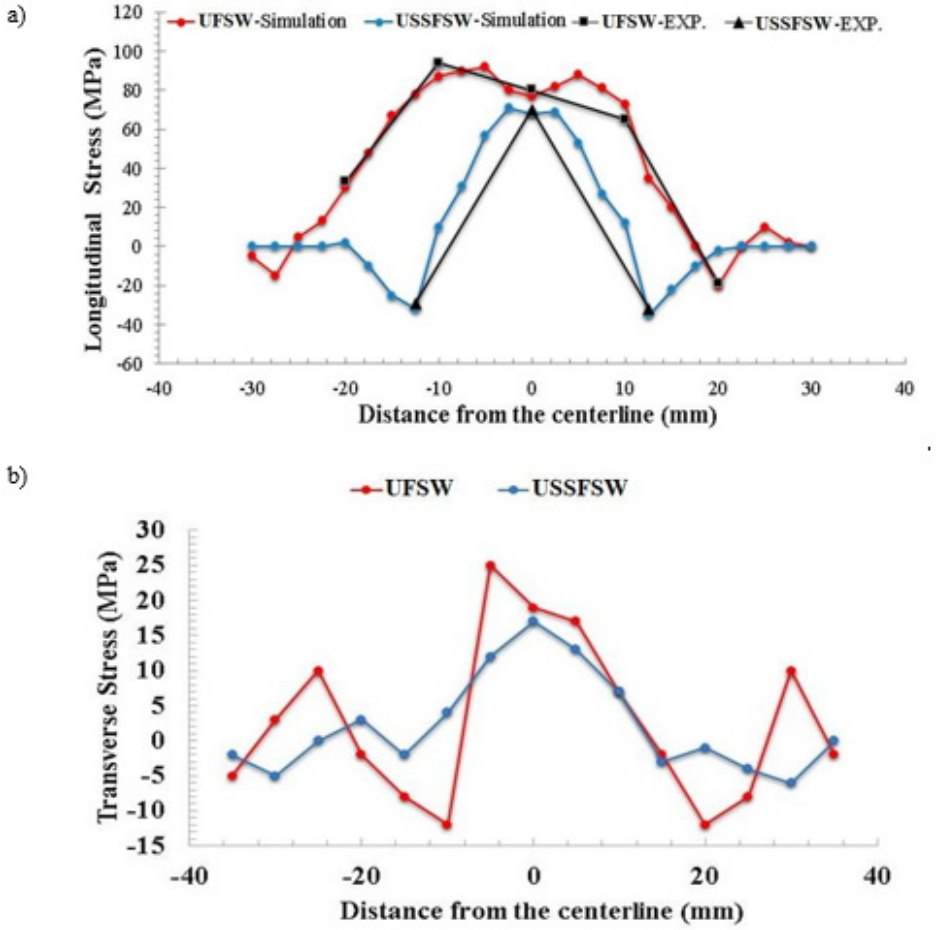

Figure 2: a) Longitudinal residual stress distribution and b) transverse residual stress distribution in the samples (with experimental and simulation methods) [13].

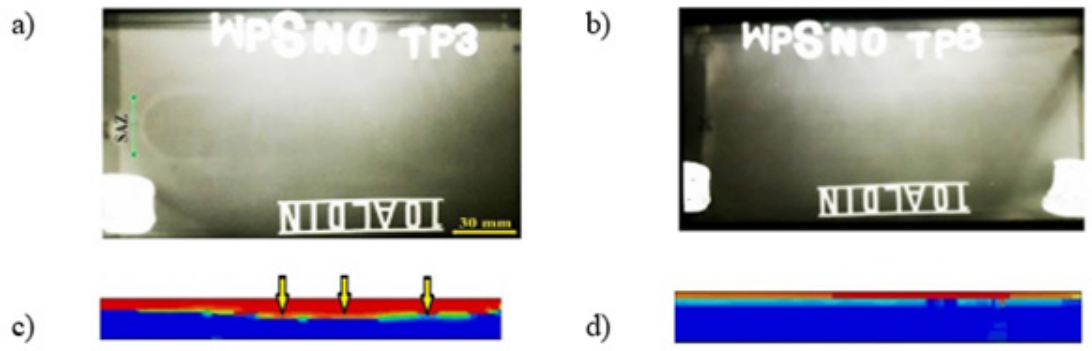

Figure 3: Detection of welding defects with the RT test, a) UFSW sample, b) USSFSW sample, and prediction of welding defects with the CEL method in c) UFSW, and d) USSFSW samples [15].

Table 1: Mechanical properties and maximum temperature measured for selected samples [7].

Sample	Elongation (%)	Yield Strength (MPa)	UTS (MPa)	Efficiency (%)	Maximum Temperature (°C)				
					Under Joint Line	AS (near surface)	RS (near surface)	AS (near bottom)	RS (near bottom)
USSFSW	6.86	235.6	282.1	91.0	404.7	329.3	328.4	321.4	322.9
UFSW	9.21	185.4	238.7	77.0	525.2	497.4	490.1	458.9	436.7

The present paper directly addresses this gap by consolidating and synthesizing the previously developed and validated CEL framework into a prescriptive design concept. Rather than presenting new experimental data, this work repurposes existing validated assets [7,13,15] to enable a paradigm shift from post-hoc analysis toward a priori process design.

The technical novelty of this article is threefold:

Synthesizing novelty: For the first time, the authors' experimentally validated CEL assets-including the temperature-dependent friction coefficient law (Equation 3), Johnson-Cook constitutive parameters (Table 2), EVF defect indicator (Figure 3) and residual stress prediction methodology (Figures 4&5)-are systematically consolidated into a unified framework with a proposed multi-objective cost function.

Table 2: Johnson-Cook constitutive parameters for AA6061-T6 obtained from Hopkinson bar testing by the authors in prior work [13].

Alloy	A	B	C	n	m	Ttransition (°K)	Tmelt (°K)
AA6061-T6	310	94	0.012	0.14	1.29	300	924

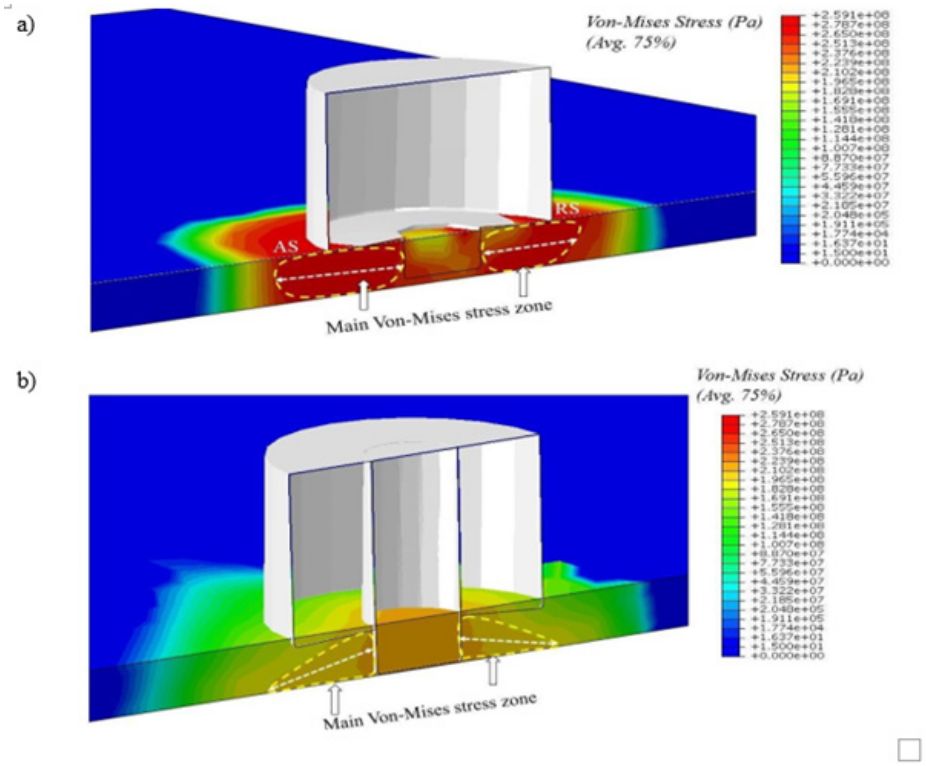

Figure 4: Three-dimensional Von-Mises stress distribution during the process obtained from CEL simulation for a) UFSW and b) USSFSW samples [13].

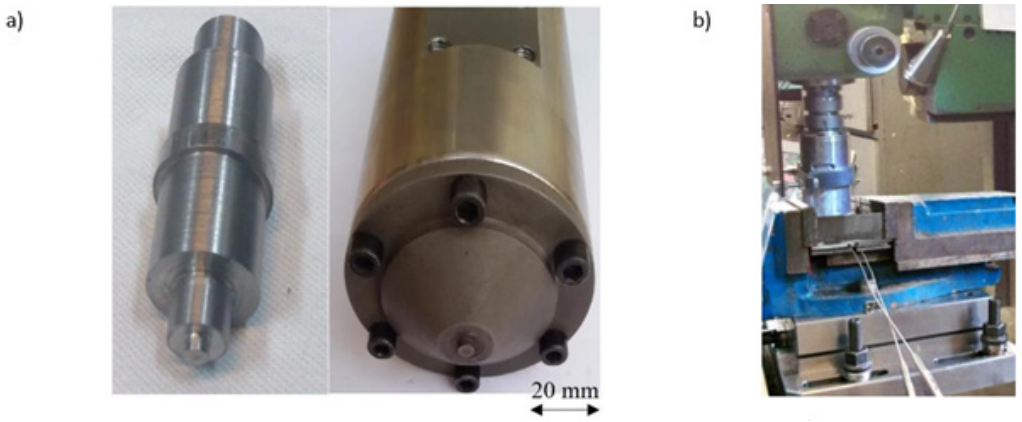

Figure 5: a) FSW tools, and b) experimental setup [13].

Methodological novelty: The validated CEL model is repurposed from an analytical instrument (explaining why USSFSW outperforms UFSW) into a proposed prescriptive design engine. This is achieved by formulating a cost function that quantifies weld quality across three simulatable metrics explicitly defined in the Methodology: (i) minimization of tensile residual stress (evaluated through simulated longitudinal stress magnitude and distribution width), (ii) maximization of post-weld strength, and (iii) defect-free integrity (assessed via EVF, where EVF<1 indicates incomplete filling).

Practical novelty: The proposed framework provides a simulation-driven pathway for future parameter optimization, eliminating reliance on costly trial-and-error campaigns-a need clearly evidenced by the baseline conditions in Table 3 (USSFSW at 2100RPM / 70mm/min vs. UFSW at 1000RPM / 70mm/min) and the observed differences in mechanical performance (Table 1) and defect formation (Figure 3).

The specific objectives and aims of this research are:

Objective 1 (Consolidation): To synthesize the previously developed and validated CEL model [13,15]-including the temperature-dependent friction law (Equation 3), Johnson-Cook parameters (Table 2), EVF defect indicator and residual stress prediction capability-into a unified computational framework.

Objective 2 (Formulation): To formulate a multi-objective cost function based on the three weld performance metrics introduced in the Methodology: (i) minimization of tensile residual stress (magnitude and distribution width from Figure 2a), (ii) maximization of post-weld strength (correlated with peak temperature reduction documented in Table 1), and (iii) defect-free integrity (EVF≥1 throughout the weld nugget, as demonstrated in Figure 3d for USSFSW).

Objective 3 (Demonstration): To demonstrate the framework's utility by comparing the two baseline conditions from prior work [7,13]-USSFSW (2100RPM, 70mm/min) and UFSW (1000RPM, 70mm/min)-and quantifying the superiority of USSFSW across thermal mitigation (peak temperature reduction from 525.2 °C to 404.7 °C), residual stress symmetry (Figures 4&5) and defect suppression (EVF analysis in Figure 3).

Importantly, this paper does not present new experimental validation of the CEL model itself-that validation was thoroughly reported in [13,15] with quantitative metrics: temperature RMSE<12 °C for USSFSW (Figure 1b), residual stress error ~9% (Figure 2a) and successful EVF-based defect prediction (Figure 3c vs. 3a for UFSW flashes). Rather, this work leverages those validated assets as a foundation for demonstrating how existing high-fidelity models can be repurposed from explanatory tools toward prescriptive design.

The remainder of this paper is organized as follows:

Section 3 presents the consolidated CEL model architecture and its prior validation (drawing on [13,15]), including the temperature-dependent friction law, Johnson-Cook constitutive model and EVF defect indicator. The results of tensile testing, temperature distribution, defect prediction, and residual stress analysis are presented and discussed in section 4. Finally, conclusions are drawn regarding the performance of USSFSW relative to UFSW, and future directions for optimization-based parameter design are proposed in section 5.

Methodology

This study integrates two previously established research streams-validated CEL simulation and experimental characterization of UFSW/USSFSW-into a unified simulation-driven optimization framework for AA6061-T6 friction stir welds. The experimental foundation draws from prior work [7,13], wherein 3-mm AA6061-T6 sheets (chemical composition and mechanical properties given in Tables 4&5) were welded using UFSW and USSFSW configurations. The conventional and stationary shoulder tools are shown in Figure 5a and the underwater experimental setup in Figure 5b. Welding parameters (Table 3) were selected to maintain equivalent power input between processes, enabling direct comparison (Tables 1&2) (Figure 5).

Table 3: Welding parameters [7].

Test Number	Rotation Speed (RPM)	Linear Speed (mm/min)	Pin Diameter (mm)
USSFSW	2100	70	5.2
UFSW	1000	70	5.2

Table 4: Chemical composition of base material [7].

Material	Mg	Mn	Si	Fe	Cr	Cu	Ti	Zn	Al
AA6061-T6	0.8	0.15	0.5	0.5	0.06	0.15	0.15	0.25	Rest

Table 5: Uniaxial tensile test results of base material [7].

Sample	Yield Strength (MPa)	Tensile Strength (MPa)	Elongation (%)	Hardness (VHN)
AA6061-T6	276	310	12	105

The numerical framework employs a Coupled Eulerian-Lagrangian (CEL) model developed in Abaqus/Explicit, rigorously validated in [15]. The workpiece is discretized as a Eulerian domain (EC3D8RT elements) to accommodate severe plastic flow, while the tool is modeled as a discrete rigid Lagrangian body (R3D4 elements). Material plasticity is defined using Johnson-Cook constitutive parameters (Table 2) obtained via Hopkinson bar testing [13]. A temperature-dependent, piecewise friction coefficient-derived from in situ force and temperature measurements-governs tool-workpiece interfacial behavior, enabling real-time updating of shear response. Thermal boundary conditions include turbulent and convective heat transfer coefficients appropriate for the underwater environment:

$$\sigma = \left[A + B\varepsilon_{pl}^{n}\right]\left[1 + C\ln\frac{\dot{\varepsilon}}{\dot{\varepsilon}_o}\right]\left[1 - T^*\right] \quad (1)$$

$$T^* = \left(\frac{T - T_{transition}}{T_{melt} - T_{transition}}\right) \quad (2)$$

The coefficients are shown in (Table 2).

Building upon this validated baseline, the present work advances the model from an analytical instrument to a prescriptive design tool. Three weld performance objectives are formalized as simulatable metrics:

A. Minimization of tensile residual stress-evaluated through simulated longitudinal stress magnitude and distribution width.

B. Maximization of post-weld strength.

C. Defect-free integrity-assessed via Eulerian Volume Fraction (EVF), where EVF<1 indicates incomplete material filling.

The CEL model is subsequently exercised across the process parameter space to identify parameter sets minimizing a multi-objective cost function encompassing these criteria. This approach constitutes a paradigm shift from simulation-as-analysis to simulation-for-control, enabling a priori optimization of weld performance without exhaustive experimental campaigns. Considering that the heat input during welding is the most important parameter affecting material flow and base metal mechanical properties, one SSFSW with stationary shoulder tool and one UFSW sample with conventional rotational tool were considered. Welding parameters are presented in Table 3. Because the heat input and material flow will be much stronger in the UFSW process. Same input power in both processes were used for compare them. For this purpose, the USSFSW sample welding parameters were selected for UFSW and only a different rotational speed was selected (Table 3).

Results and Discussion

Tensile test

Table 1 presents the results of tensile tests for USSFSW and UFSW samples. Prior to conducting the tensile tests, the expected mechanical properties were based on the anticipated reduction in peak temperature for USSFSW compared to UFSW. Because USSFSW eliminates shoulder-driven friction, the authors expected lower thermal exposure, reduced precipitate over aging, and less grain coarsening. Consequently, the expected joint efficiency for USSFSW was in the range of 85-95%, while for UFSW the expected efficiency was 70-80% [1-15]. As shown in Table 1, the experimental results (91% for USSFSW and 77% for UFSW) fell within these expected ranges, confirming that the reduced heat input in USSFSW directly translates to superior mechanical performance.

The USSFSW sample exhibits higher yield strength (235.6MPa vs. 185.4MPa) and UTS (282.1MPa vs. 238.7MPa) with superior joint efficiency (91% vs. 77%), despite lower elongation (6.86% vs. 9.21%). This strength improvement is attributed to significantly reduced peak temperatures (e.g., 404.7°C vs. 525.2°C under joint line), minimizing thermal softening and grain coarsening. The narrower, more symmetric thermal field in USSFSW produces finer, more uniform microstructure, enhancing strength at the expense of ductility (Table 1).

The lower temperatures in USSFSW reduce the extent of the heat-affected zone and limit over aging and precipitate coarsening, preserving base metal strength. Additionally, the more symmetrical temperature distribution across advancing and retreating sides promotes uniform microstructure and mechanical properties, whereas UFSW's asymmetric heating leads to localized softening and reduced joint efficiency.

Temperature distribution and temperature-dependent friction coefficient

A major limitation in existing numerical simulations of the FSW-particularly under underwater and stationary shoulder conditions-is the assumption of a constant or simplified friction coefficient at the tool-workpiece interface. Such assumptions significantly reduce prediction accuracy in thermal field evolution, material flow behavior and residual stress development. In reference [15], for the first time, a fully temperature-dependent friction coefficient model was experimentally derived and directly integrated into the CEL framework to enable dynamic control of the U-SSFSW of AA6061-T6 plates. The experimental thermal and force histories (Figure 1a) reveal five distinct thermo-mechanical stages: Pin penetration, Shoulder engagement, Dwelling, Steady-state welding (tool traverse), and Tool retraction (Figure 1).

The longitudinal temperature distribution shown in Figure 1a reveals a critical distinction between the two processes. For UFSW (upper contour plot), the thermal field exhibits a broad, teardrop-shaped high-temperature zone trailing the tool, with peak temperatures exceeding 500 °C that extend laterally toward both the advancing and retreating sides. This wide thermal footprint directly results from shoulder-driven frictional heating. In contrast, USSFSW (lower contour plot) produces a markedly narrower and more symmetric thermal field, with peak temperatures confined to approximately 400 °C immediately beneath the pin. The stationary shoulder acts as a thermal barrier rather than a heat source, creating steep thermal gradients that rapidly quench the weld zone through the surrounding water medium. Strong agreement was observed between simulation and experimental results, as shown in Figures 2b&2c. For USSFSW, the simulated thermal history matches experimental measurements with a Root-Mean-Square Error (RMSE) of less than 12 °C, accurately capturing the peak temperature of 404.7 °C and the rapid post-weld cooling. For UFSW, the simulation reproduces the higher peak temperature of 525.2 °C within a 15 °C error band, despite slightly larger variability due to asymmetric shoulder-driven flow. This validation confirms that the temperature-dependent friction law enables the CEL model to reliably predict thermal fields and, by extension, residual stresses and defect formation in both processes.

In contrast to prior models that presume a constant friction coefficient, the present study derives a temperature-dependent formulation by inserting experimentally recorded force and thermal data into the governing frictional relationships. Excluding fluctuations below a 5% threshold to preserve model stability, a piecewise expression was established across temperature intervals, as shown in Equation (3) [13]. This variable friction law was

incorporated directly into the CEL framework, enabling dynamic adjustment of interfacial shear response based on instantaneous local temperature.

$$\begin{cases} \mu = -0.041 \ln T + 0.4, & 27 \le T \le 104 \\ \mu = 0.03 \exp(0.0188T), & 104 \le T < 165 \\ \mu = -0.805 \ln T + 4.75, & 165 \le T < 276 \\ \mu = -0.0006T + 0.39, & 276 \le T \le 580 \end{cases} \quad (3)$$

[15]

The thermal field measurements reveal a substantial reduction in peak temperature for USSFSW compared to conventional UFSW. This reduction is consistently observed across all measurement locations. This pronounced thermal mitigation is attributable to the stationary shoulder configuration, which eliminates the primary heat source present in conventional FSW. In UFSW, the rotating shoulder generates extensive frictional heat across a large contact area, producing both elevated peak temperatures and a wide thermal gradient.

Conversely, USSFSW confines heat generation to the pin alone, concentrating energy input within a smaller zone while the stationary shoulder provides no frictional contribution. Although both processes employ water cooling, the reduced intrinsic heat generation in USSFSW enables more effective quenching, resulting in lower overall thermal exposure. This attenuated thermal cycle minimizes grain coarsening and precipitate dissolution, directly contributing to the superior mechanical properties and compressive residual stress state observed in USSFSW specimens.

Prediction of defects

Welding flashes and thickness reduction (denoted by white arrows in Figure 3) were observed exclusively in the UFSW specimen. These flashes arise from the outward extrusion of plasticized material under elevated thermal conditions, driven by substantial centrifugal forces within the stir-affected zone, which promote the egress of softened material [13]. The outcomes of radiographic Testing (RT) conducted on the friction stir welded joints are illustrated in Figure 3. Within the CEL framework, the Eulerian volume fraction (EVF) serves as an indicator of material occupancy within each cell: an EVF value of zero corresponds to a vacant cell, whereas a value of unity signifies complete material saturation (Figure 3).

This EVF metric offers utility in forecasting discontinuities inherent to the FSW process. Figure 3 presents the simulated EVF contours derived from the CEL approach. Although no internal cavity defects were discernible, the presence of welding flashes and attendant thickness reduction is evident in the UFSW configuration, as highlighted by yellow arrows in Figure 3. Conversely, the USSFSW configuration exhibited no indication of either flash formation or thickness diminution.

Residual stress distribution

Figure 4 shows the 3D Von-Mises stress distribution from CEL simulations of UFSW and USSFSW. UFSW stress is asymmetric, with a higher gradient on the advancing side (yellow dashed circle). The stress zone is wider near the shoulder due to its dominant role in heat generation and thermal strain; greater thermal and strain gradients increase the volume of contracted metal. Higher stress in the upper region shows that water cooling cannot offset the shoulder-induced heat. In USSFSW, the stress contour is more symmetric in both horizontal and thickness directions, reflecting the process's symmetrical nature. Lower heat input and concentrated flux around the pin reduce Von-Mises stress significantly and confine it to a smaller area.

Figure 2a shows longitudinal residual stress for USSFSW and UFSW. The model successfully prevented Eulerian material penetration into the Lagrangian domain, with good experimental-numerical agreement (max error ~9%). UFSW stress is asymmetric, with higher values on the advancing side. Residual stress in restrained FSW depends on thermal cycle [13]. In USSFSW, localized heating around the pin narrows the stress zone. Both the width of the high-temperature zone and peak temperature affect residual stress-both were reduced in USSFSW, lowering maximum stress and tensile width. Compressive stress in USSFSW is attributed to higher forging force from lower heat generation [8] (Figure 4).

Longitudinal stress differs during vs. after FSW (Figure 4 vs. 5a). Residual stress replaces compressive with tensile. This occurs because stress forms from thermal strain due to local heating/cooling. During stirring, peak temperature and gradient cause compressive stress, which relaxes after tool passage and is balanced by tensile stress. Cooling causes shrinkage of stirred metal; constraint from surrounding material generates tensile stress along the centerline. Residual stress magnitudes exceed in-process values due to increased base metal strength at lower temperatures. Figure 2b shows transverse residual stress. Values are lower than longitudinal stresses and similar between processes, indicating heat-induced transverse force is negligible relative to base metal strength [13]. USSFSW exhibits symmetric transverse stress distribution-unlike UFSW-consistent with longitudinal results. More symmetric residual stress improves mechanical properties [13] (Figure 2).

Conclusion

This study demonstrates that Underwater Stationary Shoulder Friction Stir Welding (USSFSW) significantly enhances joint strength and efficiency over conventional UFSW by reducing peak temperature and achieving symmetric thermal distribution, which minimizes softening and produces a finer, more uniform microstructure. A temperature-dependent friction law was successfully implemented in the CEL simulation, improving physical accuracy, and comparative thermal analysis confirmed that USSFSW reduces heat input by eliminating shoulder-driven friction, enabling localized thermal control. The CEL simulation effectively predicted welding flashes and thickness reduction in UFSW via EVF analysis, while USSFSW exhibited no such defects, confirming its superior material flow control and defect suppression. Furthermore, the simulation captured the asymmetric, shoulder-dominated stress distribution in UFSW and the symmetric, pin-confined stress field in USSFSW. USSFSW reduced peak temperature, narrowed the high-temperature zone, and increased forging force, leading to lower

and more symmetric residual stresses with a compressive region, thereby enhancing mechanical properties. For future applications, the validated CEL-based simulation framework can serve as a predictive digital twin for parameter optimization in thermal-sensitive alloys, reducing costly trial-and-error experimentation. This approach is particularly promising for automotive and marine industries where high-strength, distortion-free, and defect-free aluminum welds are critical.

Declarations of Statements

Conflict-of-interests

The authors have no relevant financial or non-financial interests to disclose.

Funding

No funding was received for conducting this study.

Authors' contributions

All authors contributed to the study conception and design. The first draft of the manuscript was written by Akbar hosseini based on PHD thesis and under supervision of dr Alireza Fallahi arezoudar. All authors read and approved the final manuscript.

Data and code availability

'Not Applicable'.

Supplementary information

'Not Applicable'.

Ethical approval

'Not Applicable'.

References

1. Mishra RS, Ma ZY (2005) Friction stir welding and processing. Materials Science and Engineering: R: Reports 50(1-2): 1-78.
2. Brown KH, Burns SP, Christon MA (2002) Coupled eulerian-lagrangian methods for earth penetrating weapon applications. Sandia National Laboratories, New Mexico, California, pp: 1-38.
3. Threadgill PL, Leonard AJ, Shercliff HR, Withers PJ (2009) Friction stir welding of aluminium alloys. International Materials Reviews 54(2): 49-93.
4. Zhang X, Ma Y, Li W, Huang W, Zhang W, et al. (2023) A review of residual stress effects on fatigue properties of friction stir welds. Critical Reviews in Solid State and Materials Sciences 48(6): 775-813.
5. Selvaraj M, Murali V, Koteswara Rao SR (2013) Mechanism of weld formation during friction stir welding of aluminum alloy. Materials and Manufacturing Processes 28(5): 595-600.
6. Richards DG, Prangnell PB, Williams SW, Withers PJ (2008) Global mechanical tensioning for the management of residual stresses in welds. Materials Science and Engineering: A 489(1-2): 351-362.
7. Hosseini A, Fallahi Arezoudar A (2024) Improving mechanical properties of FSWed AA6061-T6 joint by controlling microstructural changes through utilization of stationary shoulder tool in presence of Al2O3 nanoparticles and external cooling. International Journal of Precision Engineering and Manufacturing-Green Technology 11: 1163-1191.
8. Zhao Y, Wang Q, Chen H, Yan K (2014) Microstructure and mechanical properties of spray formed 7055 aluminum alloy by underwater friction stir welding. Materials & Design (1980-2015) 56: 725-730.
9. Selvaraj S, Srirangarajalu N, Kengachalam, Pranaybabu K (2024) Investigation of mechanical properties on underwater friction stir welded AA7075 with pure copper dissimilar joints. Transactions of the Indian Institute of Metals 77: 1181-1194.
10. Wu H, Chen YC, Strong D, Prangnell P (2015) Stationary shoulder FSW for joining high strength aluminum alloys. Journal of Materials Processing Technology 221: 187-196.
11. Ji SD, Meng XC, Liu JG, Zhang LG, Gao SS (2014) Formation and mechanical properties of stationary shoulder friction stir welded 6005A-T6 aluminum alloy. Materials & Design (1980-2015) 62: 113-117.
12. Baghdadchi A, Polisetti SR, Patel V, Igestrand M, Backer JD, et al. ((2026)) Stationary shoulder friction stir welding of dissimilar aluminium alloys: Microstructure and mechanical property evaluation. Welding in the World 70: 1023-1033.
13. Fallahi Arezoudar A, Hosseini A (2024) A new method for localization of the residual stress distribution and enhancement of wear resistance through underwater friction stir processing with stationary shoulder. The International Journal of Advanced Manufacturing Technology 133: 2515-2531.
14. Hosseini A, Arezoudar AF (2024) Modified CEL method for determination of defect formation mechanism in underwater stationary shoulder FSW based on softened pressure-overclosure contact relationship. Forces in Mechanics 17: 100296.
15. Hosseini A, Fallahi Arezoudar A (2023) Determining the mechanism of defect formation and material flow characteristics in underwater stationary shoulder friction stir welding using coupled Eulerian-Lagrangian simulation. The International Journal of Advanced Manufacturing Technology 127: 1755-1778.